Cluster Algorithm for Quantum Spin Chains

by

Tairan Wang

Submitted to the Department of Physics
in partial fulfillment of the requirements for the degree of

Bachelor of Science

at the

MASSACHUSETTS INSTITUTE OF TECHNOLOGY

June 1996

Author .....
Department of Physics
May 28, 1996

Certified by .....
Uwe-Jens Wiese
Assistant Professor
Thesis Supervisor

Accepted by .....
June L. Matthews
Senior Thesis Coordinator, Department of Physics

Cluster Algorithm for Quantum Spin Chains

by

Tairan Wang

Submitted to the Department of Physics
on May 28, 1996, in partial fulfillment of the
requirements for the degree of
Bachelor of Science

Abstract

In this paper, we study the formulations of loop cluster algorithms for 1D quantum spin$\frac{1}{2}$ chains. Several versions of loop cluster algorithms are then used in simulations. The study concentrates on the susceptibility χ, the staggered susceptibility χ_s, the internal energy e, and the specific heat C_v. Improved estimators are constructed for each of these quantities to reduce variations of the measurements. The results obtained with this method are shown to be in agreement with previously published results.

The specific heat of a random coupling chain is shown to be smaller in the temperature region studied than which would be required by the total entropy of the system. The missing entropy is believed to be hidden in lower temperature region. We study the specific heat of the low temperature region at $\frac{|J|}{k_B T} = 50$. There are indications of a much larger specific heat at this point than what would be given by the extrapolation of the data in the higher temperature region. However, because of the discrete Euclidean time nature of the method, the finite size effect limits the conclusiveness of the result.

It is believed that the improved estimator formulation for the specific heat can be combined with a continuous Euclidean time version of the loop cluster algorithm which will vastly improve the effectiveness of studying the low temperature region.

Thesis Supervisor: Uwe-Jens Wiese
Title: Assistant Professor

Cluster Algorithm for Quantum Spin Chains

by

Tairan Wang

Submitted to the Department of Physics
on May 28, 1996, in partial fulfillment of the
requirements for the degree of
Bachelor of Science

Abstract

In this paper, we study the formulations of loop cluster algorithms for 1D quantum spin$\frac{1}{2}$ chains. Several versions of loop cluster algorithms are then used in simulations. The study concentrates on the susceptibility χ, the staggered susceptibility χ_s, the internal energy e, and the specific heat C_v. Improved estimators are constructed for each of these quantities to reduce variations of the measurements. The results obtained with this method are shown to be in agreement with previously published results.

The specific heat of a random coupling chain is shown to be smaller in the temperature region studied than which would be required by the total entropy of the system. The missing entropy is believed to be hidden in lower temperature region. We study the specific heat of the low temperature region at $\frac{|J|}{k_B T} = 50$. There are indications of a much larger specific heat at this point than what would be given by the extrapolation of the data in the higher temperature region. However, because of the discrete Euclidean time nature of the method, the finite size effect limits the conclusiveness of the result.

It is believed that the improved estimator formulation for the specific heat can be combined with a continuous Euclidean time version of the loop cluster algorithm which will vastly improve the effectiveness of studying the low temperature region.

Thesis Supervisor: Uwe-Jens Wiese
Title: Assistant Professor

Acknowledgments

First of all, I would like to thank my advisor, Uwe-Jens Wiese, for introducing me to the world of loop clusters, and also for his invaluable teachings, advice and support. Secondly, I want to thank the thesis coordinator, June Matthews, for her patience and understanding. I also want to thank Richard Brower for the helpful discussions and pointers. Finally, I want to thank my parents for their encouragement and support in the course of my study.

Contents

List of Figures

List of Tables

Chapter 1

Introduction

Quantum spin systems are of general interest to both theorists and experimentalists. Many studies have been done on the properties of spin lattices of one or two dimensions. The system is usually described by the nearest-neighbor Heisenberg model,

$$H = \sum_{x,\mu} J_x \mathbf{S_x} \cdot \mathbf{S_{x+\mu}} \tag{1.1}$$

where $\mathbf{S_x} = \frac{1}{2}\boldsymbol{\sigma}_\mathbf{x}$ is the spin operator and J_x is the exchange coupling constant. $J_x < 0$ and $J_x > 0$ correspond to ferromagnetic and anti-ferromagnetic couplings, respectively.

The studies of two dimensional spin lattices are related to that of some high-T_c superconductors, where the undoped insulator precursors can be modeled by 2D spin systems.

One dimensional spin chains are readily available experimentally and can be studied in detail. However, pure ferromagnetic or anti-ferromagnetic systems are difficult to obtain. It is therefore of interest to study how the characteristics of pure chains extend to the case where the chains have a mixture of ferromagnetic and anti-ferromagnetic couplings.

Several analytical studies of the problem have been carried out. The solutions are highly nontrivial. On the other hand, there exist various Monte Carlo simulation algorithms that work well for 1D ferromagnets and anti-ferromagnets. Among them,

the cluster algorithms, in particular the loop cluster algorithms, work the best and are without critical slowing down experienced by local Monte Carlo algorithms. Monte Carlo simulations can provide an independent check for analytical works, and can also verify the correctness of the spin models by comparing simulation results with experimental results.

In this paper, the properties of one dimensional spin$\frac{1}{2}$ chains with random couplings (ferro or anti-ferro) of equal strength are studied by computer simulation using the loop cluster algorithms.

The study concentrates on the behavior of the susceptibility χ, the staggered susceptibility χ_s, the internal energy density e and the specific heat C_v of the system.

$$\begin{aligned} \chi &= \frac{\beta}{L}\langle(\sum_x s_x)^2\rangle \\ \chi_s &= \frac{\beta}{L}\langle(\sum_x (-1)^x s_x)^2\rangle \\ e &= \frac{1}{L}\frac{1}{Z}Tr[H\exp(-\beta H)] \\ C_v &= -\beta^2\frac{\partial e}{\partial \beta} \end{aligned} \tag{1.2}$$

In previous studies of the random coupling quantum chains, it was noticed that the specific heat of the system is lower than expected in the temperature region $k_BT/J > 0.1$. This violates the sum rule,

$$S_\infty \equiv \int_0^\infty \frac{C(T)}{T}dT = k_B \ln(2S+1) \tag{1.3}$$

which means there is missing entropy in some temperature region. It is believed that this missing entropy is in the low temperature region $k_BT/J < 0.1$. That is to say, the specific heat is expected to level off or even form a bump in low temperature region. This study attempts to study the specific heat in this low temperature region. Though there are indications of this missing entropy, the result is not conclusive. A better

algorithm should be used in order to study the low temperature region effectively.

Chapter 2

Algorithm

Quantum spin $\frac{1}{2}$ chains can be mapped into 2D systems where the additional dimension is the Euclidean time in the path integral formulation. The equivalent 2D systems can then be studied using Monte Carlo methods.[5]

2.1 Path Integral Formulation

Quantum spin chains are described by nearest-neighbor Heisenberg model, as shown in Eq(1.1). The Hamiltonian of the one-dimensional system is,

$$H = \sum_x J_x \mathbf{S_x} \cdot \mathbf{S_{x+1}} \tag{2.1}$$

where $\mathbf{S_x} = \frac{1}{2}\boldsymbol{\sigma}_\mathbf{x}$ is the spin operator. J_x is the coupling strength between spin x and spin $x+1$. If the coupling is anti-ferromagnetic, then $J_x > 0$; if it is ferromagnetic, $J_x < 0$. In this study, the magnitude of J_x is kept the same for both cases.

The partition function associated with this Hamiltonian is

$$Z = \sum_{\{S_x\}} \exp\left(-\beta H\right) = Tr \exp\left(-\beta H\right) \tag{2.2}$$

where $\beta = \frac{1}{k_B T}$ is the inverse temperature. Direct calculation is difficult since this

Hamiltonian has non-commuting terms. To circumvent this problem, we decompose the Hamiltonian into $H = H_1 + H_2$ with

$$H_1 = \sum_{x=2m-1} J_x \mathbf{S_x} \cdot \mathbf{S_{x+1}} \tag{2.3}$$

$$H_2 = \sum_{x=2m} J_x \mathbf{S_x} \cdot \mathbf{S_{x+1}} \tag{2.4}$$

Both H_1 and H_2 have only commuting terms, although they do not commute with each other. Using the Suzuki-Trotter formula, the partition function can be written as

$$Z = \lim_{N\to\infty} Tr[\exp(-\epsilon\beta H_1)\exp(-\epsilon\beta H_2)]^N \tag{2.5}$$

where $\epsilon = 1/N$ is the lattice spacing in the Euclidean time direction. By inserting complete sets of states of σ_x^z in between $\exp(-\epsilon\beta H_i)$ terms, the partition function becomes

$$Z = \lim_{N\to\infty} \sum_{\{n_i\}} \langle n_0|\exp(-\epsilon\beta H_1)|n_1\rangle\langle n_1|\exp(-\epsilon\beta H_2)|n_2\rangle$$

$$\ldots\langle n_{2N-1}|\exp(-\epsilon\beta H_2)|n_0\rangle \tag{2.6}$$

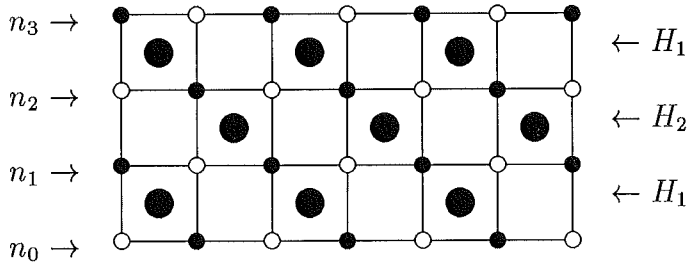

After this transformation, the partition function of the original system becomes that of a two dimensional lattice with checker-board-like 4-spin interactions. Given

the configurations $n_0, n_1, \ldots, n_{2N-1}$, the term inside the summation can be calculated. If the term is positive, then it can be interpreted as the probability of that configuration just like that in classical thermodynamics.

$$Z = \prod_{x,t} \sum_{s(x,t)=\pm 1} \exp(-S) \tag{2.7}$$

where the action is given by

$$\begin{aligned} S = & \sum_{x=2m,t=2p} S[s(x,t), s(x+1,t), s(x,t+1), s(x+1,t+1)] \\ & + \sum_{x=2m-1,t=2p-1} S[s(x,t), s(x+1,t), s(x,t+1), s(x+1,t+1)] \end{aligned} \tag{2.8}$$

the four-spin action term is related to the transfer matrix

$$\exp(-S[s_1, s_2, s_3, s_4]) = \langle s_1 s_2 | \exp(-\epsilon\beta J \mathbf{S_x} \cdot \mathbf{S_{x+1}}) | s_3 s_4 \rangle \tag{2.9}$$

2.2 Transfer Matrix

The transfer matrix is calculated for spin$\frac{1}{2}$ next.

$$\mathbf{S_x} \cdot \mathbf{S_y} = \frac{1}{4} \boldsymbol{\sigma_x} \cdot \boldsymbol{\sigma_y} = (2P_{ij} - 1)/4 \tag{2.10}$$

where P_{ij} is the permutation operator

$$P_{ij} | s_i s_j \rangle = | s_j s_i \rangle \tag{2.11}$$

$$\exp\left(-\epsilon\beta J\mathbf{S_i}\cdot\mathbf{S_j}\right)=\exp\left(\epsilon\beta J/4\right)\begin{pmatrix}1 & 0 & 0 & 0\\ 0 & \frac{1+\exp(\epsilon\beta J)}{2} & \frac{1-\exp(\epsilon\beta J)}{2} & 0\\ 0 & \frac{1-\exp(\epsilon\beta J)}{2} & \frac{1+\exp(\epsilon\beta J)}{2} & 0\\ 0 & 0 & 0 & 1\end{pmatrix} \tag{2.12}$$

For ferromagnetic coupling ($J<0$), all the terms in the transfer matrix are non-negative, and they are interpreted as probabilities of that configuration, i.e. Eq(2.9) is valid. Only six of the terms are non-zero, hence, the four-spin plaquettes can take only these six configurations.

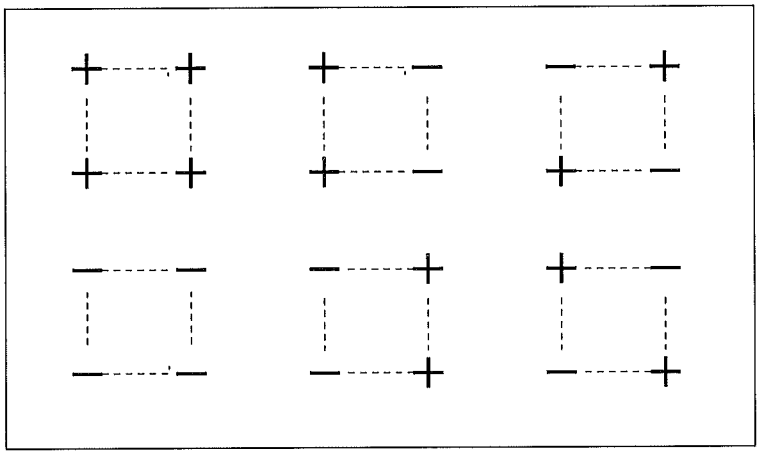

Figure 2-1: Allowed configurations for ferromagnetic plaquettes

For anti-ferromagnetic couplings ($J>0$), two terms in the matrix are negative. To use the probability interpretation, a unitary transformation is performed on every other spin,

$$U_i=\exp\left(i\frac{\pi\sigma_i^z}{2}\right)=i\sigma_i^z \tag{2.13}$$

the $\boldsymbol{\sigma}$ operators are transformed according to

$$U_i^\dagger \sigma_i^x U_i = -\sigma_i^x, \tag{2.14}$$

$$U_i^\dagger \sigma_i^y U_i = -\sigma_i^y, \tag{2.15}$$

$$U_i^\dagger \sigma_i^z U_i = \sigma_i^z \tag{2.16}$$

The transformed four-spin action is

$$S = \epsilon\beta H_{ij} = -\frac{\epsilon\beta J}{4}(2P_{ij} - 1 - 2\sigma_i^z\sigma_j^z) \tag{2.17}$$

where P_{ij} commutes with $\sigma_i^z\sigma_j^z$,

$$[P_{ij}, \sigma_i^z\sigma_j^z] = 0 \tag{2.18}$$

The transfer matrix for an anti-ferromagnetic coupling plaquette becomes

$$\exp\left(-\epsilon\beta J\mathbf{S_i}\cdot\mathbf{S_j}\right) = \exp\left(\epsilon\beta J/4\right)\begin{pmatrix} 1 & 0 & 0 & 0 \\ 0 & \frac{\exp(\epsilon\beta J)+1}{2} & \frac{\exp(\epsilon\beta J)-1}{2} & 0 \\ 0 & \frac{\exp(\epsilon\beta J)-1}{2} & \frac{\exp(\epsilon\beta J)+1}{2} & 0 \\ 0 & 0 & 0 & 1 \end{pmatrix} \tag{2.19}$$

All the terms in the transfer matrix are now non-negative and can be interpreted as probabilities. The allowed configurations for anti-ferromagnets are the same as those for ferromagnets.

2.3 Detailed Balance and the Loop Algorithm

With probability interpretation, $Z = \sum_{\{s_x\}} \exp(-\beta E_{s_x})$, all interested thermodynamic quantity can be obtained from the partition function Z.

$$\langle A \rangle = \frac{\sum_{\{s_x\}} A_{s_x} \exp(-\beta E_{s_x})}{Z} \tag{2.20}$$

To calculate Z, the entire configuration space has to be traversed. This is not practical because it usually involves a very large number of possible configurations except in minimum size systems. The Monte Carlo method samples the configuration space with the probability of sampling state S proportional to the weighting function $\exp(-\beta E_S)$. To guarantee the correctness of this sampling, the requirement of detailed balance must be satisfied[3].

$$P(i)W(i \to j) = P(j)W(j \to i) \tag{2.21}$$

where $P(i)$ is the probability of obtaining state i and $W(i \to j)$ is the transition probability from state i to state j of the algorithm used, i.e., the probability of obtaining state j next given that the current state is i. $P(i)$ for all the allowed configurations are listed in Table(2.1).

Solving the linear equation group Eq(2.21), the transition probabilities are shown in Table(2.2). All the other transition terms that are not included in Table(2.2) equal to zero.

Table 2.1: Relative probabilities of states, $P(i)$

Type	label	Configuration,i	P(i)
Ferro	C1	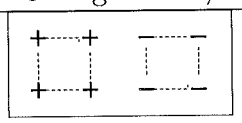	1
	C2	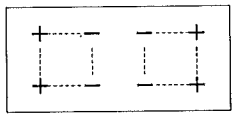	$\frac{1+\exp(\epsilon\beta J)}{2}$
	C3	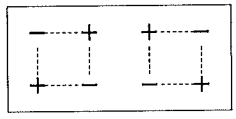	$\frac{1-\exp(\epsilon\beta J)}{2}$
Anti	C1	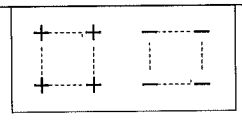	1
	C2	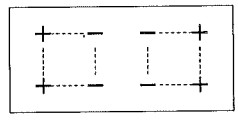	$\frac{\exp(\epsilon\beta J)+1}{2}$
	C3	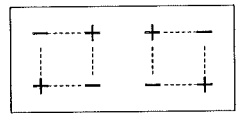	$\frac{\exp(\epsilon\beta J)-1}{2}$

Table 2.2: Transition probabilities. $w1 = \frac{1+exp(-\epsilon\beta J)}{2}$, and $w2 = \frac{2}{1+exp(\epsilon\beta J)}$

Ferro	$C1 \rightarrow C2$	$w1$
	$C1 \rightarrow C3$	$1 - w1$
	$C2 \rightarrow C1$	1
	$C3 \rightarrow C1$	1
Anti	$C1 \rightarrow C2$	1
	$C2 \rightarrow C1$	$w2$
	$C2 \rightarrow C3$	$1 - w2$
	$C3 \rightarrow C1$	1

Figure 2-2: State transition diagram

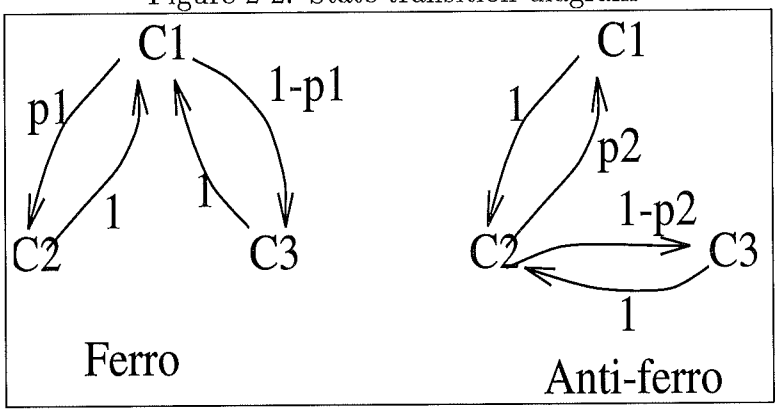

With the weightings of the states and the transition probabilities between them determined, the loop algorithm is constructed to generate new patterns. At each lattice point, a flow direction determines where the next point in the loop should be. For ferromagnets, the flow patterns are given as,

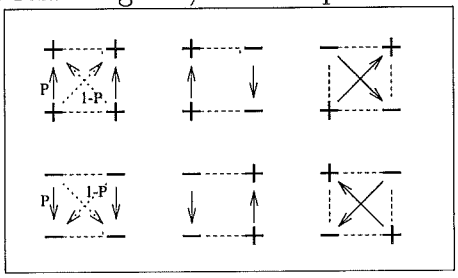

where $p = \frac{1+\exp(-\epsilon\beta J)}{2}$.

For anti-ferromagnets, the flow patterns are,

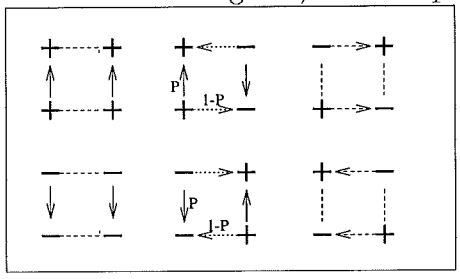

where $p = \frac{2}{1+\exp(\epsilon\beta J)}$.

To generate a loop, a starting point is chosen. Then, the loop is generated by following the flow pattern. Since there are a finite number of lattice sites, and the pattern configurations forbid three prone path,

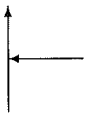

the loop is guaranteed to close. It is easily verified that this procedure satisfies the detailed balance requirement outlined earlier.

For the multi-loop algorithm, the simulation starts with an initial configuration that consists of allowed four-spin plaquette terms. One easy starting point is uniform up-spins (or down-spins). Loops are generated according to the given procedure. The procedure guarantees that each spin is in one and only one loop. When all the loops are generated, each loop is then flipped (all the spins in that loop are flipped) with 50% probability. Measurements of interested quantities of the lattice are performed before the next cycle of loop-generation starts.

Several thousand cycles are used to put the system into thermal equilibrium before a large number of cycles with measurements are done to accumulate data.

2.4 Characteristic Quantities of the System

As mentioned in the introduction Eq(1.2), we are interested in studying the susceptibility χ, the staggered susceptibility χ_s, the internal energy density e and the specific heat C_v of the system.

The measurement of χ and χ_s can be done based on the formula directly.

For the internal energy density,

$$\begin{aligned} e &= \frac{1}{L}\frac{1}{Z}Tr[H\exp(-\beta H)] \\ &= -\frac{1}{L}\frac{1}{Z}\frac{\partial Z}{\partial \beta} \end{aligned} \tag{2.22}$$

the partition function is

$$Z = \prod_x \sum_{S_x=\pm 1} \exp(-S_x) \tag{2.23}$$

and the derivative of the partition function is

$$\begin{aligned} \frac{\partial Z}{\partial \beta} &= \prod_x \sum_{S_x=\pm 1} \frac{\partial}{\partial \beta} \exp(-S_x) \\ &= \prod_x \sum_{S_x=\pm 1} (-\frac{\partial S_x}{\partial \beta}) \exp(-S_x) \\ &= -Z\langle \frac{\partial S_x}{\partial \beta} \rangle \end{aligned} \tag{2.24}$$

hence, the internal energy is

$$e = \frac{1}{L}\langle \frac{\partial S}{\partial \beta} \rangle \tag{2.25}$$

Following the same line of thought, the specific heat can be expressed in a similar fashion,

$$\begin{aligned} C_v &= -\beta^2 \frac{\partial e}{\partial \beta} \\ &= \frac{\beta^2}{LZ}[\frac{\partial^2}{\partial \beta^2} Z - \frac{1}{Z}(\frac{\partial Z}{\partial \beta})^2] \end{aligned} \tag{2.26}$$

the second derivative of Z is

$$\frac{\partial^2 Z}{\partial \beta^2} = \prod_x \sum_{S_x=\pm 1} (-\frac{\partial^2 S_x}{\partial \beta^2} + (\frac{\partial S_x}{\partial \beta})^2) \exp(-S_x)$$
$$= Z\langle -\frac{\partial^2 S}{\partial \beta^2} + (\frac{\partial S}{\partial \beta})^2 \rangle \tag{2.27}$$

the specific heat is

$$C_v = \frac{\beta^2}{L}[-\langle \frac{\partial^2 S}{\partial \beta^2} \rangle + \langle (\frac{\partial S}{\partial \beta})^2 \rangle - \langle \frac{\partial S}{\partial \beta} \rangle^2] \tag{2.28}$$

where $\langle \ldots \rangle$ is the average over all configurations.

In the ferromagnetic case, the probabilities (Boltzmann factors) are

$$\exp(-S_1) = \exp(-\epsilon \beta J/4) \tag{2.29}$$

$$\exp(-S_2) = \exp(-\epsilon \beta J/4) \frac{1 + \exp(\epsilon \beta J)}{2} \tag{2.30}$$

$$\exp(-S_3) = \exp(-\epsilon \beta J/4) \frac{1 - \exp(\epsilon \beta J)}{2} \tag{2.31}$$

From these equation, we obtain,

$$\frac{\partial S_1}{\partial \beta} = -\exp(S_1)\frac{\partial}{\partial \beta}\exp(-S_1) \tag{2.32}$$
$$= -\exp(\epsilon\beta J/4)\frac{\partial}{\partial \beta}\exp(-\epsilon\beta J/4)$$
$$= \epsilon J/4$$
$$\frac{\partial S_2}{\partial \beta} = -\exp(S_2)\frac{\partial}{\partial \beta}\exp(-S_2) \tag{2.33}$$
$$= -\frac{2\exp(\epsilon\beta J/4)}{1+\exp(\epsilon\beta J)}\frac{\partial}{\partial \beta}[\exp(-\epsilon\beta J/4)\frac{(1+\exp(\epsilon\beta J))}{2}]$$
$$= \frac{\epsilon J}{4}\cdot\frac{1-3\exp(\epsilon\beta J)}{1+\exp(\epsilon\beta J)}$$
$$\frac{\partial S_3}{\partial \beta} = -\exp(S_3)\frac{\partial}{\partial \beta}\exp(-S_3) \tag{2.34}$$
$$= -\frac{2\exp(\epsilon\beta J/4)}{1-\exp(\epsilon\beta J)}\frac{\partial}{\partial \beta}[\exp(-\epsilon\beta J/4)\frac{(1-\exp(\epsilon\beta J))}{2}]$$
$$= \frac{\epsilon J}{4}\cdot\frac{1+3\exp(\epsilon\beta J)}{1-\exp(\epsilon\beta J)}$$

the second derivatives are obtained to be,

$$\frac{\partial^2 S_1}{\partial \beta^2} = 0 \tag{2.35}$$
$$\frac{\partial^2 S_2}{\partial \beta^2} = -(\epsilon J)^2\frac{\exp(\epsilon\beta J)}{[1+\exp(\epsilon\beta J)]^2} \tag{2.36}$$
$$\frac{\partial^2 S_3}{\partial \beta^2} = (\epsilon J)^2\frac{\exp(\epsilon\beta J)}{[1-\exp(\epsilon\beta J)]^2} \tag{2.37}$$

For the anti-ferromagnetic case, the calculations give exactly the same results for $\frac{\partial S_i}{\partial \beta}$ and $\frac{\partial^2 S_i}{\partial \beta^2}$, but with $J = 1$ instead of $J = -1$ which is for ferromagnets.

2.5 Improved Estimators

In the loop algorithm described in section(2.4), only one half of the loops will be flip in each cycle, on average. By using the literal ways of measuring χ and χ_s, the auto-

correlations between successive measurements are high and the standard deviations are large.

The idea behind the improved estimator is to explicitly average over a subset of the variable space and take the results as independent data[6].

$$\langle A \rangle = \frac{\sum_{\phi,\phi_s} \exp\left(-S(\phi,\phi_s)\right) A_{\phi,\phi_s}}{\sum_{\phi,\phi_s} \exp\left(-S(\phi,\phi_s)\right)} \tag{2.38}$$

where ϕ_s can be explicitly averaged out. Let

$$A_{improve} = \frac{\sum_{\phi_s} \exp\left(-S(\phi,\phi_s)\right) A_{\phi,\phi_s}}{\sum_{\phi_s} \exp\left(-S(\phi,\phi_s)\right)} \tag{2.39}$$

then $A_{improve}$ is treated as independent data, and we have

$$\langle A \rangle = \langle A_{improve} \rangle = \frac{\sum_{\phi} A_{improve}}{\sum_{\phi}} \tag{2.40}$$

$$\sigma_A \geq \sigma_{A_{improve}}$$

2.5.1 Susceptibility and Staggered Susceptibility

For the susceptibility,

$$\chi = \frac{\beta}{L} \langle (\sum_x s_x)^2 \rangle \tag{2.41}$$

$$\langle \mathfrak{M}^2 \rangle \equiv \langle (\sum_x s_x)^2 \rangle = \langle (\sum_\zeta \mathfrak{M}_\zeta)^2 \rangle$$

where ζ is the loop index and $\mathfrak{M}_\zeta = \sum_{x \in \zeta} s_x$

$$\langle \mathfrak{M}^2 \rangle = \langle \sum_{\zeta 1 \zeta 2} \mathfrak{M}_{\zeta_1} \mathfrak{M}_{\zeta_2} \rangle$$

but $\langle \mathfrak{M}_{\zeta 1} \mathfrak{M}_{\zeta 2} \rangle = 0$ unless $\zeta 1 = \zeta 2$ [1],

[1] $\mathfrak{M}_\zeta$ will take either one value or its negative. $\mathfrak{M}_{\zeta 1} = m_1, or\ -m_1; \mathfrak{M}_{\zeta 2} = m_2, or\ -m_2$.

hence

$$\langle \mathfrak{M}^2 \rangle = \langle \sum_{\zeta} \mathfrak{M}_{\zeta}{}^2 \rangle$$

therefore, the susceptibility is

$$\chi = \frac{\beta}{L} \langle (\sum_{\zeta} \mathfrak{M}_{\zeta})^2 \rangle \tag{2.42}$$

The staggered susceptibility can be expressed similarly as,

$$\chi_s = \frac{\beta}{L} \langle (\sum_{\zeta} \mathfrak{M}s_{\zeta})^2 \rangle \tag{2.43}$$

where $\mathfrak{M}s = \sum_x (-1)^x s_x$.

From the improved estimator formulae for χ and χ_s, we see that the measurements are done through individual loops, hence there exists the option of doing a single-loop algorithm instead of the multi-loop algorithm. In a single-loop algorithm, only one loop that passes through a randomly chosen starting point is generated in each cycle. In doing so, more longer loops are generated. The probability is proportional to the length of the loop. The susceptibility is then given by,

$\langle \mathfrak{M}_{\zeta 1} \mathfrak{M}_{\zeta 2} \rangle = (m_1 m_2 + m_1(-m_2) + (-m_1)m_2 + (-m_1)(-m_2))/4 = 0.$

$$\chi = \frac{\beta}{L}\langle\frac{L\cdot 2N}{|\zeta|}(\mathfrak{M}_\zeta)^2\rangle$$
$$= 2N\beta\langle\frac{(\mathfrak{M}_\zeta)^2}{|\zeta|}\rangle \tag{2.44}$$

similarly for the staggered susceptibility,

$$\chi_s = 2N\beta\langle\frac{(\mathfrak{M}s_\zeta)^2}{|\zeta|}\rangle \tag{2.45}$$

2.5.2 Internal Energy Density

It is shown in section(2.4) that $e = \frac{1}{L}\langle\frac{\partial S}{\partial\beta}\rangle$. $\frac{\partial S}{\partial\beta}$ depends on the four-spin-interaction plaquettes instead of on single spins like $\mathfrak{M}$ does.

Let E be a shorthand to $\frac{\partial S}{\partial\beta}$

$$E = \sum_i E_i,\ i \text{ is the plaquette index}$$
$$= \sum_\zeta E_\zeta \tag{2.46}$$

where E_ζ is the contribution of loop ζ to the total. If loop ζ goes through a particular plaquette i twice, then this plaquette contributes its E_i to E_ζ alone; otherwise, E_i is evenly split between the two loops going through plaquette i.

Then the average of E is,

$$\langle E\rangle = \langle\sum_\zeta E_\zeta\rangle \tag{2.47}$$

given a particular loop configuration.

If there are N loops, each can be flipped or not. Average over the sub-ensemble

of all 2^N configurations,

$$\langle E \rangle = \langle \sum_{\zeta} \overline{E_\zeta} \rangle \tag{2.48}$$

$$\overline{E_\zeta} = \sum_{i \in \zeta} \overline{E_i} \tag{2.49}$$

For each plaquette, if it belongs to a single loop, then E_i takes only one value in all 2^N configurations: $\overline{E_i} = E_i$. Otherwise, $\overline{E_i} = \frac{1}{2}(E_i^{(1)} + E_i^{(2)})$. Since both $E_i^{(k)}$s can be measured given the current 4-spin configuration and the loop flow pattern, we can obtain the average $\overline{E_\zeta}$, without generating all the configurations involved.

In the actual program, $\overline{E_\zeta}$ is generated as the loop is being followed through. Plaquettes are marked as their contributions, $\frac{1}{4}(E_i^{(1)} + E_i^{(2)})$, are included into $\overline{E_\zeta}$. When and if it is detected that a previously marked plaquette is included again, this means that E_i belongs to loop ζ alone, and the correction is added: $E_i^{(1)} - \frac{1}{4}(E_i^{(1)} + E_i^{(2)}) = \frac{1}{4}(3E_i^{(1)} - E_i^{(2)})$.

The internal energy density is then,

$$e = \frac{1}{L} \langle \sum_{\zeta} \overline{E_\zeta} \rangle \tag{2.50}$$

Similar to the case of susceptibility, the multi-loop algorithm procedure can be converted to be used in a single-loop algorithm. Instead of summing over all loops, $\langle \sum_\zeta \overline{E_\zeta} \rangle$, only one loop is measured each time. The weighting factor is the same as that of χ for the same reason that longer loops have a higher chance of being selected.

$$\langle E \rangle = \langle \frac{2NL}{|\zeta|} \overline{E_\zeta} \rangle \tag{2.51}$$

and the internal energy density will be

$$e = \frac{2N}{|\zeta|} \langle \overline{E_\zeta} \rangle \tag{2.52}$$

2.5.3 Specific Heat

The improved estimator of the specific heat is more difficult to obtain than those of the others.

As shown in section(2.4),

$$C_v = \frac{\beta^2}{L}[-\langle \frac{\partial^2 S}{\partial \beta^2} \rangle + \langle (\frac{\partial S}{\partial \beta})^2 \rangle - \langle \frac{\partial S}{\partial \beta} \rangle^2]. \tag{2.53}$$

$\langle \frac{\partial S}{\partial \beta} \rangle^2$ can be obtained directly from the energy measurement. $\langle \frac{\partial^2 S}{\partial \beta^2} \rangle$ can be measured same way $\langle \frac{\partial S}{\partial \beta} \rangle$ is. However, $\langle (\frac{\partial S}{\partial \beta})^2 \rangle$ needs more work.

$$\begin{aligned} \langle E^2 \rangle &= \langle (\sum_\zeta E_\zeta)^2 \rangle \\ &= \langle (\sum_{\zeta 1, \zeta 2} E_{\zeta 1, \zeta 2})^2 \rangle \end{aligned} \tag{2.54}$$

where $E_{\zeta 1, \zeta 2} = \sum_{plaquette\ k \in \zeta_1, \zeta_j} E_k/2$,

$$= \langle \sum_{\zeta 1, \zeta 2; \zeta 3, \zeta 4} E_{\zeta 1, \zeta 2} E_{\zeta 3, \zeta 4} \rangle \tag{2.55}$$

Taking the average over a loop configuration the same way as that in the case of

internal energy density,

$$\begin{aligned}\langle E^2\rangle &= \langle \overline{E^2}\rangle \\ &= \langle \sum_{\zeta 1,\zeta 2;\zeta 3,\zeta 4} \overline{E_{\zeta 1,\zeta 2}E_{\zeta 3,\zeta 4}}\rangle \end{aligned} \tag{2.56}$$

where $\overline{E_{\zeta 1,\zeta 2}E_{\zeta 3,\zeta 4}}$ is the average over the sub-ensemble of all 2^N configurations.

There are several cases to consider.

If $\zeta 1 = \zeta 2$, then

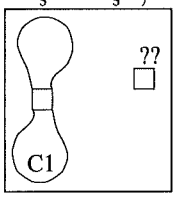

$$\begin{aligned}\overline{E_{\zeta 1,\zeta 1}E_{??}} &= E_{\zeta 1,\zeta 1}\overline{E_{??}} \\ &= \overline{E_{\zeta 1,\zeta 1}}\cdot\overline{E_{??}}\end{aligned} \tag{2.57}$$

since $E_{\zeta 1,\zeta 1}$ is independent of loops' orientations. $E_{??}$ means that the loops involved do not matter.

If $\zeta 1 = \zeta 4$, then

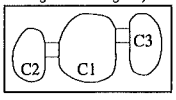

let $E^+_{\zeta 1,\zeta 2}$ be the value when $\zeta 1$ and $\zeta 2$ have the same orientations (the direction of a loop is chosen arbitrarily). $E^-_{\zeta 1,\zeta 2}$ is the value when they have the opposite orientations.

$$\begin{aligned}\overline{E_{\zeta 1,\zeta 2}E_{\zeta 1,\zeta 3}} &= \frac{1}{4}(E^+_{\zeta 1,\zeta 2}E^+_{\zeta 1,\zeta 3} + E^+_{\zeta 1,\zeta 2}E^-_{\zeta 1,\zeta 3} + E^-_{\zeta 1,\zeta 2}E^+_{\zeta 1,\zeta 3} + E^-_{\zeta 1,\zeta 2}E^-_{\zeta 1,\zeta 3}) \\ &= (\frac{E^+_{\zeta 1,\zeta 2} + E^-_{\zeta 1,\zeta 2}}{2})(\frac{E^+_{\zeta 1,\zeta 3} + E^-_{\zeta 1,\zeta 3}}{2}) \\ &= \overline{E_{\zeta 1,\zeta 2}}\cdot\overline{E_{\zeta 1,\zeta 3}}\end{aligned} \tag{2.58}$$

If $\zeta 1, \zeta 2, \zeta 3, \zeta 4$ are all distinct,

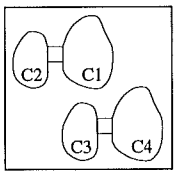

all four loops can take any orientations independently,

$$\overline{E_{\zeta 1,\zeta 2}E_{\zeta 3,\zeta 4}} = \overline{E_{\zeta 1,\zeta 2}} \cdot \overline{E_{\zeta 3,\zeta 4}} \tag{2.59}$$

The last case is if $\zeta 1 = \zeta 3$, and $\zeta 2 = \zeta 4$, then

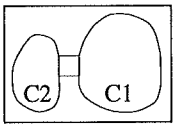

$$\overline{E_{\zeta 1,\zeta 2}E_{\zeta 1,\zeta 2}} = \frac{1}{2}[(E^{+}_{\zeta 1,\zeta 2})^2 + (E^{-}_{\zeta 1,\zeta 2})^2] \tag{2.60}$$

$$= \overline{E_{\zeta 1,\zeta 2}} \cdot \overline{E_{\zeta 1,\zeta 2}} + \Delta_{\zeta 1,\zeta 2} \tag{2.61}$$

where

$$\Delta_{\zeta 1,\zeta 2} = \overline{E^2_{\zeta 1,\zeta 2}} - \overline{E_{\zeta 1,\zeta 2}}^2 \tag{2.62}$$

$$= (\frac{E^{+}_{\zeta 1,\zeta 2} - E^{-}_{\zeta 1,\zeta 2}}{2})^2$$

Except for the last case, we have $\overline{E_{\zeta 1,\zeta 2}E_{\zeta 3,\zeta 4}} = \overline{E_{\zeta 1,\zeta 2}} \cdot \overline{E_{\zeta 3,\zeta 4}}$.

Therefore,

$$\sum_{\zeta 1,\zeta 2;\zeta 3,\zeta 4} \overline{E_{\zeta 1,\zeta 2}E_{\zeta 3,\zeta 4}} = \sum_{\cdots} \overline{E_{\zeta 1,\zeta 2}} \cdot \overline{E_{\zeta 3,\zeta 4}} + 2 \sum_{\zeta 1,\zeta 2} \Delta_{\zeta 1,\zeta 2}$$

$$= (\sum_{\zeta 1,\zeta 2} \overline{E_{\zeta 1,\zeta 2}})^2 + 2 \sum_{\zeta 1,\zeta 2} \Delta_{\zeta 1,\zeta 2} \tag{2.63}$$

but

$$\overline{E_{\zeta 1}} = \sum_{\zeta 2} \overline{E_{\zeta 1,\zeta 2}} \tag{2.64}$$

hence

$$\sum_{\zeta 1,\zeta 2} \overline{E_{\zeta 1,\zeta 2}} = \sum_{\zeta} \overline{E_{\zeta}} \tag{2.65}$$

$$\langle E^2 \rangle = \langle \sum_{\zeta 1,\zeta 2} (\overline{E_{\zeta 1}} \cdot \overline{E_{\zeta 2}} + 2\Delta_{\zeta 1,\zeta 2}) \rangle \tag{2.66}$$

The single loop modification that works for χ, and e does not extend to the case of specific heat easily. The reason is that specific heat depends on the interaction between two plaquettes, which involves four loops instead of two in the case of χ and e. The closest analogy is a two-loop implementation.

At each cycle, two loops are randomly generated. Note that the starting points are randomly chosen, so the two could be the same loop. From the multi-loop version of the improved estimator, we see that

$$\overline{E^2} = \sum_{\zeta 1,\zeta 2} (\overline{E_{\zeta 1}} \cdot \overline{E_{\zeta 2}} + 2\Delta_{\zeta 1,\zeta 2})$$

By choosing the starting points randomly, the probability of measuring term $\zeta 1, \zeta 2$ is $\frac{|\zeta 1| \cdot |\zeta 2|}{(2NL)^2}$. Similar to the case in single-loop,

$$\langle E \rangle = \langle \overline{E^2} \rangle = \langle W_{\zeta 1,\zeta 2} (\overline{E_{\zeta 1}} \cdot \overline{E_{\zeta 2}} + 2\Delta^2_{\zeta 1 \zeta 2}) \rangle \tag{2.67}$$

where $W_{\zeta 1,\zeta 2} = \frac{(2NL)^2}{|\zeta 1| \cdot |\zeta 2|}$.

2.6 Analytical Studies of Small Systems

To provide an independent check for the loop algorithm, some small systems are studied analytically. For a short chain with only two or four spins, it is possible to evaluate the transition matrices directly. Therefore, exact expressions of susceptibility and specific heat can be found.

2.6.1 Susceptibility of a 2-spin System

Recall that the partition function can be written as,

$$Z = \lim_{N\to\infty} \sum_{\{n_i\}} \langle n_0| \exp(-\epsilon\beta H_1)|n_1\rangle \langle n_1| \exp(-\epsilon\beta H_2)|n_2\rangle$$

$$\ldots \langle n_{2N-1}| \exp(-\epsilon\beta H_2)|n_0\rangle \tag{2.68}$$

In this case, there are only two spins, with periodic condition.

$$\hat{H}_1 = J\hat{S}_0 \cdot \hat{S}_1 \tag{2.69}$$

$$\hat{H}_2 = J\hat{S}_1 \cdot \hat{S}_0 \tag{2.70}$$

Hence, $\hat{H}_1 = \hat{H}_2$

$$\chi = \frac{\beta}{L}\langle \mathfrak{M}^2 \rangle \tag{2.71}$$

and $\langle \mathfrak{M}^2 \rangle$ can be written as,

$$Z \cdot \langle \mathfrak{M}^2 \rangle = \frac{1}{2N} \sum_{i=0}^{2N-1} \hat{\mathfrak{M}}\hat{T}^i \hat{\mathfrak{M}}\hat{T}^{2N-i} \tag{2.72}$$

where $\hat{T} = \exp(-\epsilon\beta\hat{H}_1) = \exp(-\epsilon\beta\hat{H}_2)$.

Choose the basis as $|\uparrow\uparrow\rangle$, $|\uparrow\downarrow\rangle$, $|\downarrow\uparrow\rangle$ and $|\downarrow\downarrow\rangle$, then

$$T = A \begin{pmatrix} 1 & 0 & 0 & 0 \\ 0 & \frac{1+s}{2} & \frac{1-s}{2} & 0 \\ 0 & \frac{1-s}{2} & \frac{1+s}{2} & 0 \\ 0 & 0 & 0 & 1 \end{pmatrix} \tag{2.73}$$

where $s = \exp(\epsilon\beta J)$, and $A = \exp(\epsilon\beta J/4)$

Under the chosen basis, the $\hat{\mathfrak{M}}_z$ operator is given by

$$\hat{\mathfrak{M}}_z = \hat{S}_{0z} + \hat{S}_{1z} = \begin{pmatrix} 1 & 0 & 0 & 0 \\ 0 & 0 & 0 & 0 \\ 0 & 0 & 0 & 0 \\ 0 & 0 & 0 & -1 \end{pmatrix} \tag{2.74}$$

The staggered susceptibility is given by

$$\hat{\mathfrak{M}}_{sz} = \hat{S}_{0z} - \hat{S}_{1z} = \begin{pmatrix} 0 & 0 & 0 & 0 \\ 0 & 1 & 0 & 0 \\ 0 & 0 & -1 & 0 \\ 0 & 0 & 0 & 0 \end{pmatrix} \tag{2.75}$$

Diagonalize the transfer matrix, and the new basis is $|\uparrow\uparrow\rangle$, $\frac{|\uparrow\downarrow\rangle+|\downarrow\uparrow\rangle}{\sqrt{2}}$, $\frac{|\uparrow\downarrow\rangle-|\downarrow\uparrow\rangle}{\sqrt{2}}$, and $|\downarrow\downarrow\rangle$.

$$T = A \begin{pmatrix} 1 & 0 & 0 & 0 \\ 0 & 1 & 0 & 0 \\ 0 & 0 & s & 0 \\ 0 & 0 & 0 & 1 \end{pmatrix} \tag{2.76}$$

and

$$T^i = A^i \begin{pmatrix} 1 & 0 & 0 & 0 \\ 0 & 1 & 0 & 0 \\ 0 & 0 & s^i & 0 \\ 0 & 0 & 0 & 1 \end{pmatrix} \tag{2.77}$$

$$\mathfrak{M}_z = \hat{S}_{0z} + \hat{S}_{1z} = \begin{pmatrix} 1 & 0 & 0 & 0 \\ 0 & 0 & 0 & 0 \\ 0 & 0 & 0 & 0 \\ 0 & 0 & 0 & -1 \end{pmatrix} \tag{2.78}$$

$$\mathfrak{M}_{sz} = \hat{S}_{0z} - \hat{S}_{1z} = \begin{pmatrix} 0 & 0 & 0 & 0 \\ 0 & 0 & 1 & 0 \\ 0 & 1 & 0 & 0 \\ 0 & 0 & 0 & 0 \end{pmatrix} \tag{2.79}$$

Then Eq(2.72) gives,

$$Z \cdot \langle \mathfrak{M}^2 \rangle = Tr \frac{1}{2N} \sum_{i=0}^{2N-1} A^{2N} \begin{pmatrix} 1 & 0 & 0 & 0 \\ 0 & 0 & 0 & 0 \\ 0 & 0 & 0 & 0 \\ 0 & 0 & 0 & -1 \end{pmatrix} \begin{pmatrix} 1 & 0 & 0 & 0 \\ 0 & 1 & 0 & 0 \\ 0 & 0 & s^i & 0 \\ 0 & 0 & 0 & 1 \end{pmatrix} \begin{pmatrix} 1 & 0 & 0 & 0 \\ 0 & 0 & 0 & 0 \\ 0 & 0 & 0 & 0 \\ 0 & 0 & 0 & 1 \end{pmatrix} \begin{pmatrix} 1 & 0 & 0 & 0 \\ 0 & 1 & 0 & 0 \\ 0 & 0 & s^{2N-i} & 0 \\ 0 & 0 & 0 & 1 \end{pmatrix}$$

$$= 2 \exp\left(-\frac{\beta J}{2}\right) \tag{2.80}$$

For the staggered susceptibility,

$$Z \cdot \langle \mathfrak{M}_s^2 \rangle = Tr \frac{1}{2N} \sum_{i=0}^{2N-1} A^{2N} \begin{pmatrix} 0 & 0 & 0 & 0 \\ 0 & 0 & 1 & 0 \\ 0 & 1 & 0 & 0 \\ 0 & 0 & 0 & 0 \end{pmatrix} \begin{pmatrix} 1 & 0 & 0 & 0 \\ 0 & 1 & 0 & 0 \\ 0 & 0 & s^i & 0 \\ 0 & 0 & 0 & 1 \end{pmatrix} \begin{pmatrix} 0 & 0 & 0 & 0 \\ 0 & 0 & 1 & 0 \\ 0 & 1 & 0 & 0 \\ 0 & 0 & 0 & 0 \end{pmatrix} \begin{pmatrix} 1 & 0 & 0 & 0 \\ 0 & 1 & 0 & 0 \\ 0 & 0 & s^{2N-i} & 0 \\ 0 & 0 & 0 & 1 \end{pmatrix}$$

$$= \frac{A^{2N}}{2N} \cdot \frac{(1+s)(1-s^{2N})}{1-s} \tag{2.81}$$

The partition function is

$$Z = Tr(T^{2N}) = Tr A^{2N} \begin{pmatrix} 1 & 0 & 0 & 0 \\ 0 & 1 & 0 & 0 \\ 0 & 0 & s^{2N} & 0 \\ 0 & 0 & 0 & 1 \end{pmatrix} = A^{2N}(3 + s^{2N}) \tag{2.82}$$

The susceptibilities are then given by

$$\chi = \frac{\beta}{L} \langle \mathfrak{M}^2 \rangle = \frac{\beta}{L} \cdot \frac{2}{3 + \exp(2\beta J)} \tag{2.83}$$

$$\chi_s = \frac{\beta}{L} \langle \mathfrak{M}_s^2 \rangle = \frac{\beta}{L} \cdot \frac{1 - \exp(2\beta J)}{3 + \exp(2\beta J)} \cdot \frac{1 + \exp(\epsilon \beta J)}{2N(2 - \exp(\epsilon \beta J))} \tag{2.84}$$

$\|s4, s3, s2, s1\rangle$	$\hat{H}\|s4, s3, s2, s1\rangle$
$\|\uparrow\uparrow\uparrow\uparrow\rangle$	$\|\uparrow\uparrow\uparrow\uparrow\rangle$
$\|\downarrow\downarrow\downarrow\downarrow\rangle$	$\|\downarrow\downarrow\downarrow\downarrow\rangle$
$\|\uparrow\uparrow\uparrow\downarrow\rangle$	$(\|\downarrow\uparrow\uparrow\uparrow\rangle + \|\uparrow\uparrow\downarrow\uparrow\rangle)/2$
$\|\uparrow\uparrow\downarrow\uparrow\rangle$	$(\|\uparrow\downarrow\uparrow\uparrow\rangle + \|\uparrow\uparrow\uparrow\downarrow\rangle)/2$
$\|\uparrow\downarrow\uparrow\uparrow\rangle$	$(\|\uparrow\uparrow\downarrow\uparrow\rangle + \|\downarrow\uparrow\uparrow\uparrow\rangle)/2$
$\|\downarrow\uparrow\uparrow\uparrow\rangle$	$(\|\uparrow\uparrow\uparrow\downarrow\rangle + \|\uparrow\downarrow\uparrow\uparrow\rangle)/2$
$\|\downarrow\downarrow\downarrow\uparrow\rangle$	$(\|\uparrow\downarrow\downarrow\downarrow\rangle + \|\downarrow\downarrow\uparrow\downarrow\rangle)/2$
$\|\downarrow\downarrow\uparrow\downarrow\rangle$	$(\|\downarrow\uparrow\downarrow\downarrow\rangle + \|\downarrow\downarrow\downarrow\uparrow\rangle)/2$
$\|\downarrow\uparrow\downarrow\downarrow\rangle$	$(\|\downarrow\downarrow\uparrow\downarrow\rangle + \|\uparrow\downarrow\downarrow\downarrow\rangle)/2$
$\|\uparrow\downarrow\downarrow\downarrow\rangle$	$(\|\downarrow\downarrow\downarrow\uparrow\rangle + \|\downarrow\uparrow\downarrow\downarrow\rangle)/2$
$\|\uparrow\uparrow\downarrow\downarrow\rangle$	$(\|\uparrow\downarrow\uparrow\downarrow\rangle + \|\downarrow\uparrow\downarrow\uparrow\rangle)/2$
$\|\downarrow\uparrow\uparrow\downarrow\rangle$	$(\|\uparrow\downarrow\uparrow\downarrow\rangle + \|\downarrow\uparrow\downarrow\uparrow\rangle)/2$
$\|\downarrow\downarrow\uparrow\uparrow\rangle$	$(\|\uparrow\downarrow\uparrow\downarrow\rangle + \|\downarrow\uparrow\downarrow\uparrow\rangle)/2$
$\|\uparrow\downarrow\downarrow\uparrow\rangle$	$(\|\uparrow\downarrow\uparrow\downarrow\rangle + \|\downarrow\uparrow\downarrow\uparrow\rangle)/2$
$\|\uparrow\downarrow\uparrow\downarrow\rangle$	$(\|\uparrow\uparrow\downarrow\downarrow\rangle + \|\downarrow\downarrow\uparrow\uparrow\rangle + \|\downarrow\downarrow\uparrow\uparrow\rangle + \|\uparrow\downarrow\downarrow\uparrow\rangle)/2 - \|\uparrow\downarrow\uparrow\downarrow\rangle$
$\|\downarrow\uparrow\downarrow\uparrow\rangle$	$(\|\uparrow\uparrow\downarrow\downarrow\rangle + \|\downarrow\uparrow\uparrow\downarrow\rangle + \|\downarrow\downarrow\uparrow\uparrow\rangle + \|\uparrow\downarrow\downarrow\uparrow\rangle)/2 - \|\downarrow\uparrow\downarrow\uparrow\rangle$

Table 2.3: Matrix component of the 4-spin system

2.6.2 Specific Heat of a 4-spin System

We use a 4-spin chain system to demonstrate the analytical calculation of specific heat.

$$\begin{aligned}\hat{H} &= J\mathbf{S_1}\cdot\mathbf{S_2} + \mathbf{S_2}\cdot\mathbf{S_3} + \mathbf{S_3}\cdot\mathbf{S_4} + \mathbf{S_4}\cdot\mathbf{S_1} \\ &= J[\frac{1}{2}(S_{1+}S_{2-} + S_{2+}S_{3-} + S_{3+}S_{4-} + S_{4+}S_{1-} + S_{1-}S_{2+} + S_{2-}S_{3+} + S_{3-}S_{4+} + S_{4-}S_{1+}) \\ &\qquad + (S_{1z}S_{2z} + S_{2z}S_{3z} + S_{3z}S_{4z} + S_{4z}S_{1z})] \qquad (2.85)\end{aligned}$$

where $S_z|\uparrow\rangle = \frac{1}{2}|\uparrow\rangle$, $S_+|\downarrow\rangle = |\uparrow\rangle$, and $S_-|\uparrow\rangle = |\downarrow\rangle$.

The matrix components are shown in Table(2.3). Diagonalize the matrix and the eigenstates and eigenvectors are as shown in Table(2.4).

the eigenvalues are J, J, J, $-J$, 0, 0, J, $-J$, 0, 0, J, $-J$, $-2J$, 0, 0, 0,

Eigenstates	Eigenvalues
$\|\uparrow\uparrow\uparrow\uparrow\rangle$	J
$\|\downarrow\downarrow\downarrow\downarrow\rangle$	J
$(\|\uparrow\uparrow\uparrow\downarrow\rangle + \|\uparrow\uparrow\downarrow\uparrow\rangle + \|\uparrow\downarrow\uparrow\uparrow\rangle + \|\downarrow\uparrow\uparrow\uparrow\rangle)/2$	J
$(\|\uparrow\uparrow\uparrow\downarrow\rangle - \|\uparrow\uparrow\downarrow\uparrow\rangle + \|\uparrow\downarrow\uparrow\uparrow\rangle - \|\downarrow\uparrow\uparrow\uparrow\rangle)/2$	$-J$
$(\|\uparrow\uparrow\uparrow\downarrow\rangle - \|\uparrow\downarrow\uparrow\uparrow\rangle)/\sqrt{2}$	0
$(\|\uparrow\uparrow\downarrow\uparrow\rangle - \|\downarrow\uparrow\uparrow\uparrow\rangle)/\sqrt{2}$	0
$(\|\downarrow\downarrow\downarrow\uparrow\rangle + \|\downarrow\downarrow\uparrow\downarrow\rangle + \|\downarrow\uparrow\downarrow\downarrow\rangle + \|\uparrow\downarrow\downarrow\downarrow\rangle)/2$	J
$(\|\downarrow\downarrow\downarrow\uparrow\rangle - \|\downarrow\downarrow\uparrow\downarrow\rangle + \|\downarrow\uparrow\downarrow\downarrow\rangle - \|\uparrow\downarrow\downarrow\downarrow\rangle)/2$	$-J$
$(\|\downarrow\downarrow\downarrow\uparrow\rangle - \|\downarrow\uparrow\downarrow\downarrow\rangle)/\sqrt{2}$	0
$(\|\downarrow\downarrow\uparrow\downarrow\rangle - \|\uparrow\downarrow\downarrow\downarrow\rangle)/\sqrt{2}$	0
$(2\|\uparrow\downarrow\uparrow\downarrow\rangle + 2\|\downarrow\uparrow\downarrow\uparrow\rangle - \|\uparrow\uparrow\downarrow\downarrow\rangle - \|\downarrow\uparrow\uparrow\downarrow\rangle - \|\downarrow\downarrow\uparrow\uparrow\rangle - \|\uparrow\downarrow\downarrow\uparrow\rangle)/2\sqrt{3}$	$-2J$
$(\|\uparrow\downarrow\uparrow\downarrow\rangle - \|\downarrow\uparrow\downarrow\uparrow\rangle)/2\sqrt{3}$	$-J$
$(\|\uparrow\uparrow\downarrow\downarrow\rangle - \|\uparrow\downarrow\downarrow\uparrow\rangle)/\sqrt{2}$	0
$(\|\downarrow\downarrow\uparrow\uparrow\rangle - \|\downarrow\uparrow\uparrow\downarrow\rangle)/\sqrt{2}$	0
$(\|\uparrow\uparrow\downarrow\downarrow\rangle - \|\downarrow\uparrow\uparrow\downarrow\rangle - \|\downarrow\downarrow\uparrow\uparrow\rangle + \|\uparrow\downarrow\downarrow\uparrow\rangle)/2$	0
$(\|\uparrow\uparrow\downarrow\downarrow\rangle + \|\downarrow\uparrow\uparrow\downarrow\rangle + \|\downarrow\downarrow\uparrow\uparrow\rangle + \|\uparrow\downarrow\downarrow\uparrow\rangle + \|\uparrow\downarrow\uparrow\downarrow\rangle + \|\downarrow\uparrow\downarrow\uparrow\rangle)/\sqrt{6}$	J

Table 2.4: Eigenstates and eigenvalues of the 4-spin system

Hence, the partition function is,

$$\begin{aligned} Z &= Tr(\exp(-\beta H)) \\ &= 7 + 5\exp(-\beta J) + 3\exp(\beta J) + \exp(2\beta J) \end{aligned} \tag{2.86}$$

and

$$\frac{\partial Z}{\partial \beta} = J(-5\exp(-\beta J) + 3\exp(\beta J) + 2\exp(2\beta J)) \tag{2.87}$$

$$\frac{\partial^2 Z}{\partial \beta^2} = J^2(5\exp(-\beta J) + 3\exp(\beta J) + 4\exp(2\beta J)) \tag{2.88}$$

The specific heat is found to be,

$$C_v = \frac{\beta^2}{LZ}[\frac{\partial^2 Z}{\partial \beta^2} - \frac{1}{Z}(\frac{\partial Z}{\partial \beta})^2] \tag{2.89}$$
$$= \frac{\beta^2 J^2}{L}[\frac{35\exp(-\beta J) + 60 + 66\exp(\beta J) + 28\exp(2\beta J) + 3\exp(3\beta J)}{(7 + 5\exp(-\beta J) + 3\exp(\beta J) + \exp(2\beta J))^2}]$$

Chapter 3

Data and Analysis

3.1 Correctness Studies

3.1.1 Susceptibility and Staggered Susceptibility of a 2-spin System

The susceptibilities of the 2-spin system are as shown in Eq(2.84).

$$\chi = \frac{\beta}{L} \cdot \frac{2}{3 + \exp(2\beta J)} \tag{3.1}$$

$$\chi_s = \frac{\beta}{L} \cdot \frac{1 - \exp(2\beta J)}{3 + \exp(2\beta J)} \cdot \frac{1 + \exp(\epsilon\beta J)}{2N(1 - \exp(\epsilon\beta J))} \tag{3.2}$$

The susceptibility is independent of N–the granularity of the Euclidean time direction. The results from the loop algorithm calculation for $2N = 64$ are plotted against the theoretical curve in Figure(3-1) and Figure(3-2).

The staggered susceptibility, however, does depend on the granularity. This dependency is verified as shown by the plots of the loop algorithm results along with the theoretical curves in Figure(3-3) and Figure(3-4).

As can be seen from the figures, the results obtained from the loop algorithm calculation are in agreement with the theoretical results within one standard deviation.

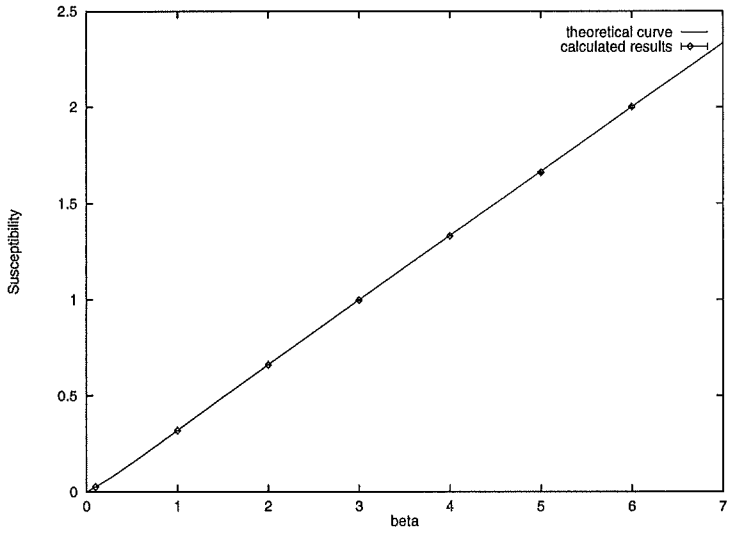

Figure 3-1: Susceptibility for 2-spin ferromagnetic chain

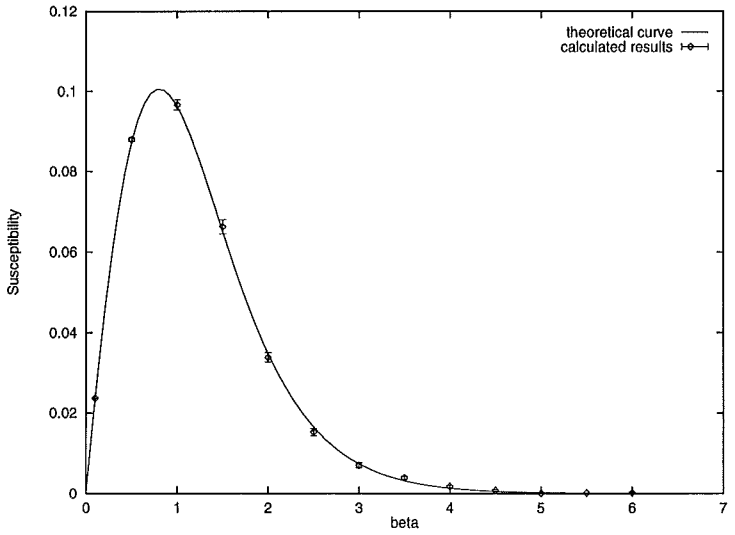

Figure 3-2: Susceptibility for 2-spin anti-ferromagnetic chain

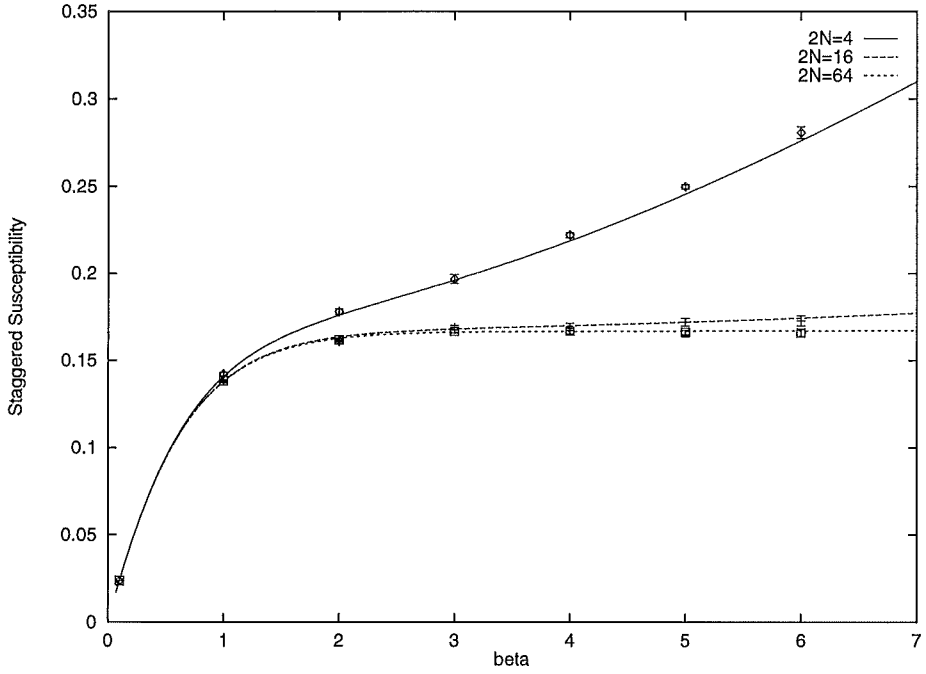

Figure 3-3: Staggered susceptibility for 2-spin ferromagnetic chain

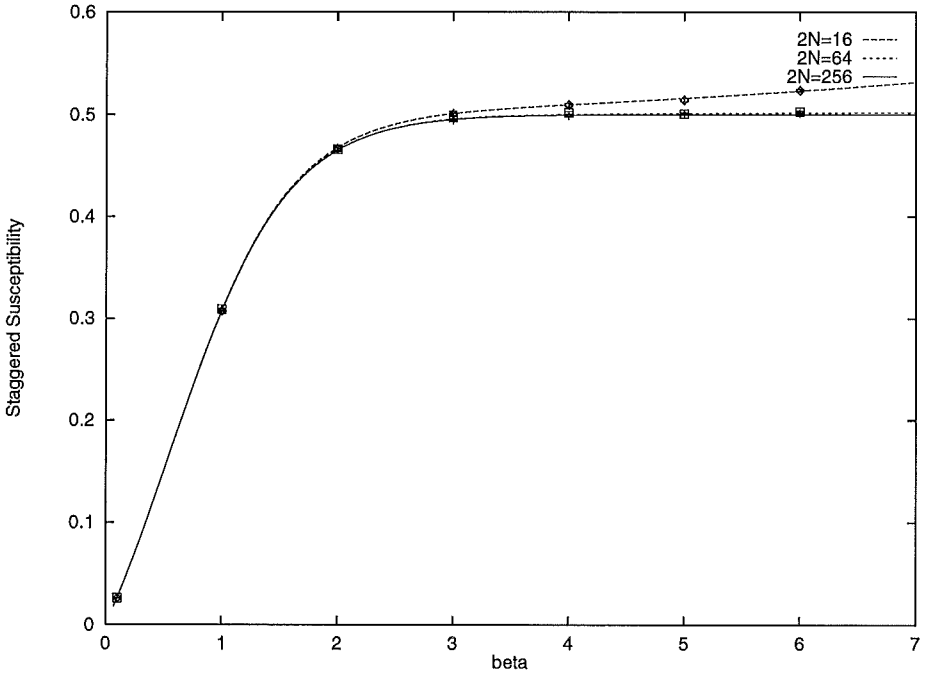

Figure 3-4: Staggered susceptibility for 2-spin anti-ferromagnetic chain

3.1.2 Specific Heat of a 4-spin System

The equation for the specific heat of a 4-spin system is given in Eq(2.90).

The theoretical prediction is plotted together with the simulation results obtained from the loop algorithm program in Figure(3-5). Again, the results from the program agree closely with the theoretical curve.

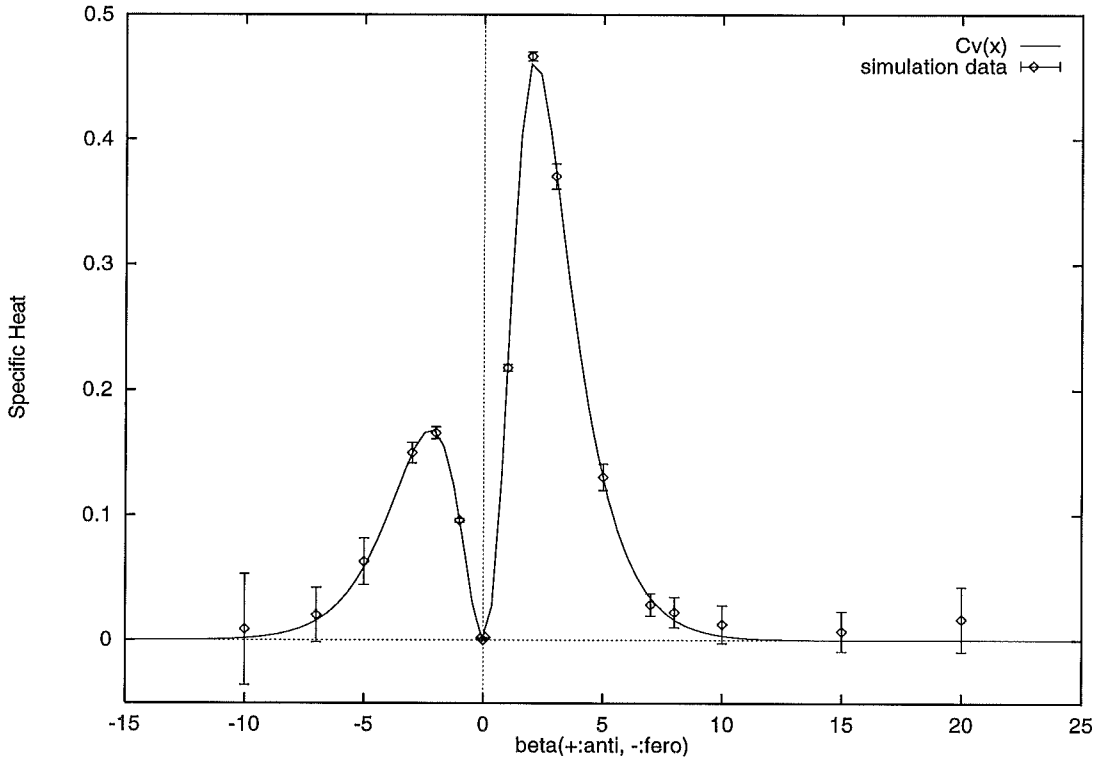

Figure 3-5: Specific heat for a 4-spin system of ferro and anti-ferromagnetic couplings

Table 3.1: Results for one-dimensional spin chains.

J	β	L	$2N$	χ	χ_s	e	$\chi_{s.f.}$[a]
1	1	32	32	0.137(1)	0.381(1)	-0.205(2)	0.421(2)
1	1	32	64	0.138(1)	0.381(1)	-0.200(2)	0.420(2)
1	1	32	128	0.137(1)	0.380(1)	-0.202(2)	0.427(2)
1	1	32	256	0.136(1)	0.383(1)	-0.203(2)	0.432(2)
1	2	128	16	0.144(1)	0.979(3)	-0.344(1)	1.244(6)
1	4	128	32	0.126(1)	2.323(10)	-0.424(1)	3.505(15)
1	8	128	64	0.115(1)	5.146(28)	-0.441(1)	8.43(3)
1	16	128	16	0.070(1)	28.17(16)	-0.591(1)	47.66(16)
1	16	128	32	0.100(1)	14.54(9)	-0.490(1)	25.56(8)
1	16	128	64	0.110(1)	11.74(8)	-0.455(1)	22.07(7)
1	16	128	128	0.114(1)	11.21(8)	-0.445(1)	20.48(7)
-1	1	32	32	0.367(1)	0.151(1)	-0.134(1)	0.184(1)
-1	1	32	64	0.366(1)	0.151(1)	-0.134(1)	0.179(1)
-1	1	32	128	0.366(1)	0.152(1)	-0.133(1)	0.179(1)
-1	1	32	256	0.369(1)	0.150(1)	-0.134(1)	0.175(1)
-1	2	128	16	0.932(3)	0.198(1)	-0.188(1)	0.330(1)
-1	4	128	32	2.534(8)	0.206(1)	-0.221(1)	0.665(2)
-1	8	128	64	7.302(26)	0.192(1)	-0.238(1)	1.342(2)
-1	16	128	16	19.21(7)	0.243(2)	-0.247(1)	2.604(5)
-1	16	128	32	21.59(8)	0.194(1)	-0.245(1)	2.661(4)
-1	16	128	64	22.64(9)	0.180(1)	-0.245(1)	2.656(4)
-1	16	128	128	22.69(9)	0.176(1)	-0.245(1)	2.680(4)

[a] χ_s is defined as $\frac{\beta}{L}(\sum_x(-1)^x s(x,t_0))$ in the paper [2], which is called structure factor $\chi_{s.f.}$ here.

3.1.3 Susceptibility and Internal Energy of Many Spin Systems

Longer chains are studied using a single-loop version of the algorithm. The results are listed in Table(3.1).

The results obtained are in agreement with data obtained from previous studies done by Uwe-Jens Wiese using block cluster algorithm[2].

3.2 Random Coupling Chains

The previous section has concentrated on establishing the correctness of the program. This section turns to the case of random coupling chains.

3.2.1 Susceptibility

The susceptibilities of several different chain configurations are plotted in Figure(3-6).[1] The dependencies on temperature of χ of pure ferromagnets, pure anti-ferromagnets and random coupling cases are qualitatively what we expected.

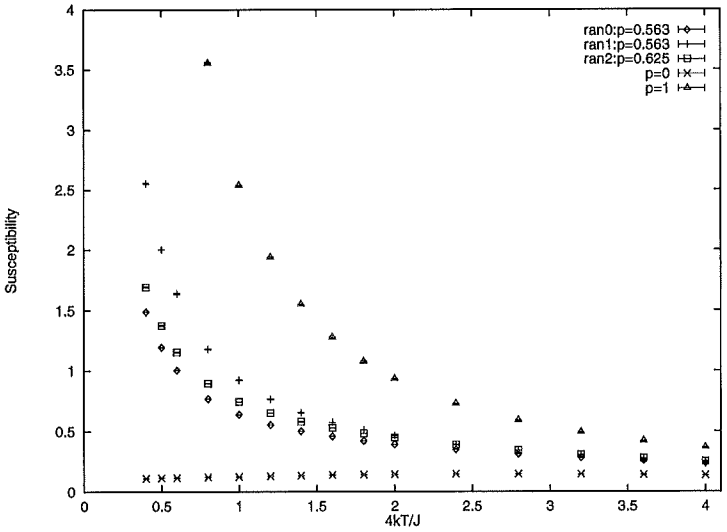

Figure 3-6: Susceptibility for 32-spin chains. $p = 1$ is ferromagnetic, $p = 0$ is anti-ferromagnetic, and $p \in [0..1]$ is random couplings

The staggered susceptibilities χ_s exhibit similar behaviors as the susceptibilities χ. The difference is that the relative strength of the ferromagnets and that of the anti-ferromagnets is reversed. See Figure(3-7).

[1] Of the three random coupling cases, ran0 has configuration AFFFAAAFAFAFFAFFAFFAA-FAAFFFFFAFA; ran1 has configuration FAAAFFAAFFAAFFFFFFAFFFAAAAFFFFAA; ran2 has configuration AFFAFFFFAFAFFFFAFAAFFAAAFAAFFFFF;

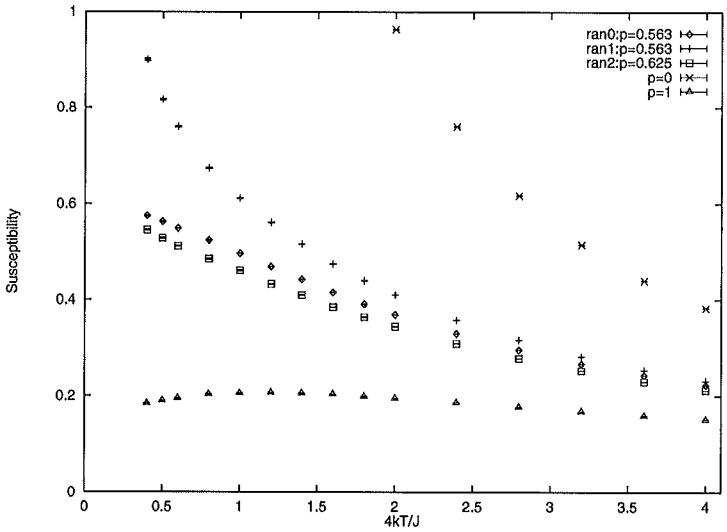

Figure 3-7: Staggered Susceptibility for 32-spin chains. $p = 1$ is ferromagnetic, $p = 0$ is anti-ferromagnetic, and $p \in [0..1]$ is random couplings

3.2.2 Specific Heat

The specific heat results are plotted in Figure(3-8). p is the probability of a coupling to be ferromagnetic. The results are in agreement with the results obtained from earlier studies using transfer matrix calculation and high temperature series method[1].

As can be seen from the plot, the specific heat of $0 < p < 1$ cases are always below that of the anti-ferromagnets in the temperature region studied $0.1 < k_B T/|J| < 1$. If this trend can be extrapolated to the lower temperature region, then according to Eq(1.3), the entropy calculated for the random coupling case will be smaller than what it should be.

The assumption is that the missing entropy can be found in lower temperature region where low-energy excitations would contribute to make up for this lost entropy.

However, when the temperature is below $k_B T/|J| = 0.1$, the current loop algorithms suffer from finite size effect[2].

[2]The Suzuki-Trotter formula requires that the granularity of the Euclidean time goes to zero. $\epsilon \to 0$, $N \to \infty$. The program can only use finite N, which leads to a deviation from the limiting case. This is the finite size effect that limits the usefulness of the current algorithm in low temperature region.

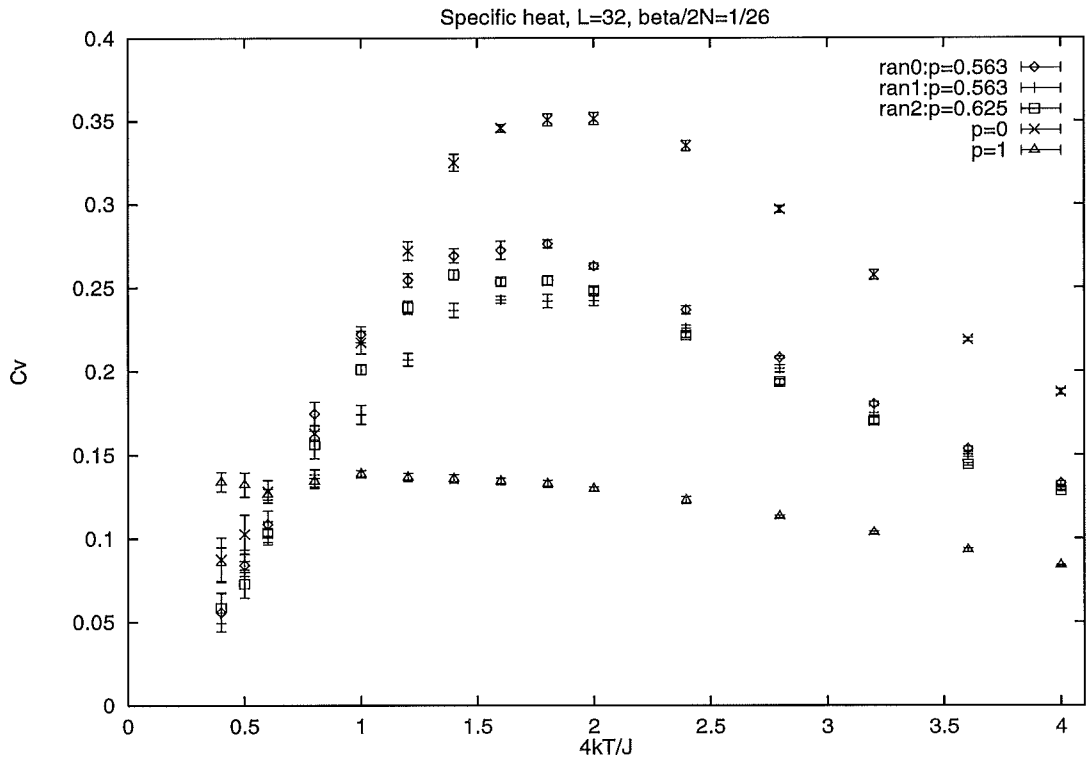

Figure 3-8: Specific heat for 32-spin chains, with $p \in [0, 1]$. $p = 0$ is anti-ferromagnet; $p = 1$ is ferromagnet.

Nevertheless, an effort is made to measure the specific heat of random coupling chains at $\frac{|J|}{k_B T} = 50$. Dozens of measurements are done with different parameters. The lengths of the chains range from 8 to 64, and the total number of segments in the Euclidean time direction ranges from 50 to 1500. As can be seen from the data plots in Figure(3-9), for $\beta = 50$, $2N > 500$ is needed to avoid severe finite size effects. It is also noted that the exact configuration of the chain has important effect on the result.

Several runs result in widely different specific heat results, as can be seen from the two data point at $2N = 1500$ in Figure(3-9). Since it is theorized that the low temperature excitations contribute to the larger than extrapolated specific heat, and that these excitations are closely associated with boundaries between ferro- and anti-ferro segments, the particular configuration involved may influence the specific heat drastically, i.e. a simple percentage count of ferromagnetic couplings will not be sufficient to describe the system. If this is the case, then more measurements taking into account the weighted contribution of the whole configuration assembly must be performed to reach a conclusion of the low temperature specific heat of random coupling chains.

The computation time of a single-loop/two-loop algorithm is proportional to the size of the 2D system. For a multi-loop algorithm, either the computation time is proportional to the size of the system squared, or both the memory storage and the computation time are proportional to the size of the system. The need for large $2N$ in low temperature region and large L to encompass more of the configuration space make it computationally expensive to use the current algorithms.

3.3 Loop Statistics

Several flavors of the loop cluster algorithm generate new configurations with different weights on different sizes of loops.

With the multi-loop algorithm, there are more small loops generated than large loops. The single and two loop versions of the algorithm, however, put higher weight on larger loops in generating new configurations.

Figure 3-9: Specific heat of random coupling chains at $\frac{|J|}{k_B T} = 50$

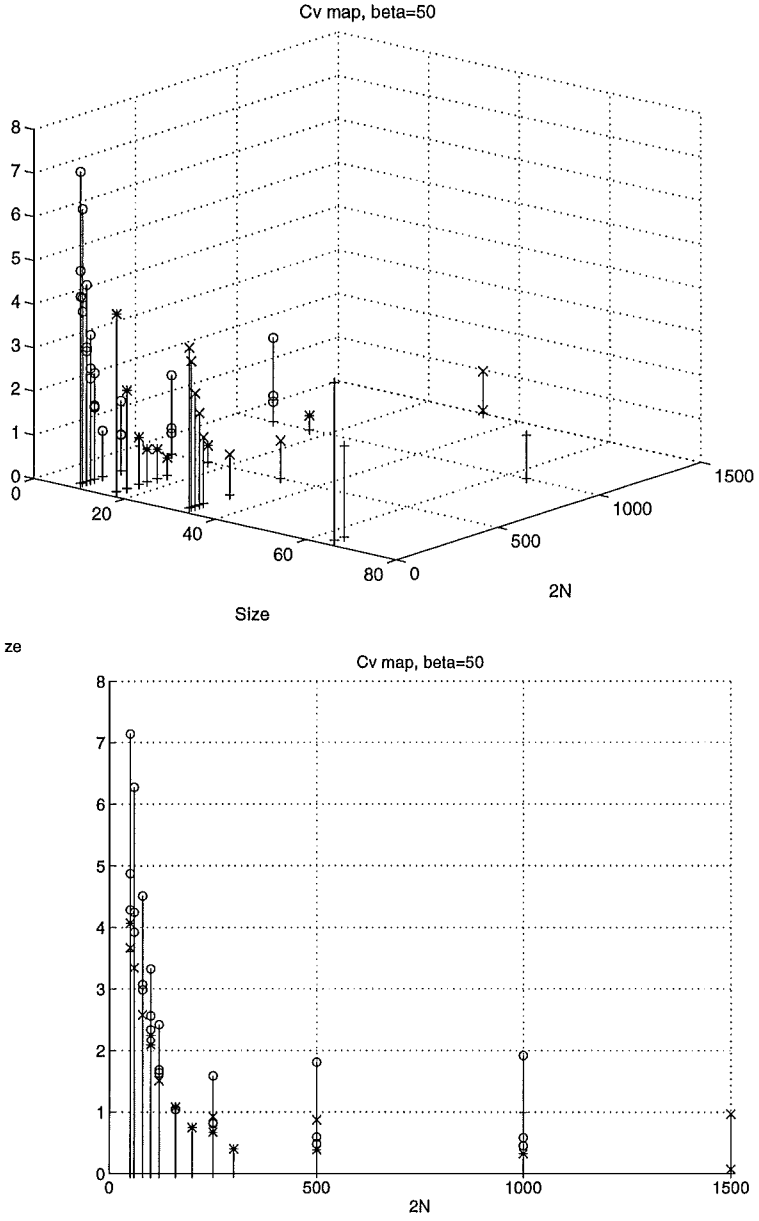

Both of these observations are verified in our studies, as shown in Figure(3-10). The loop population of a multi-loop algorithm has an exponential dependency on the loop length. When two-loop algorithm is used. More longer loops are generated, which show up as the shoulder in the figure.

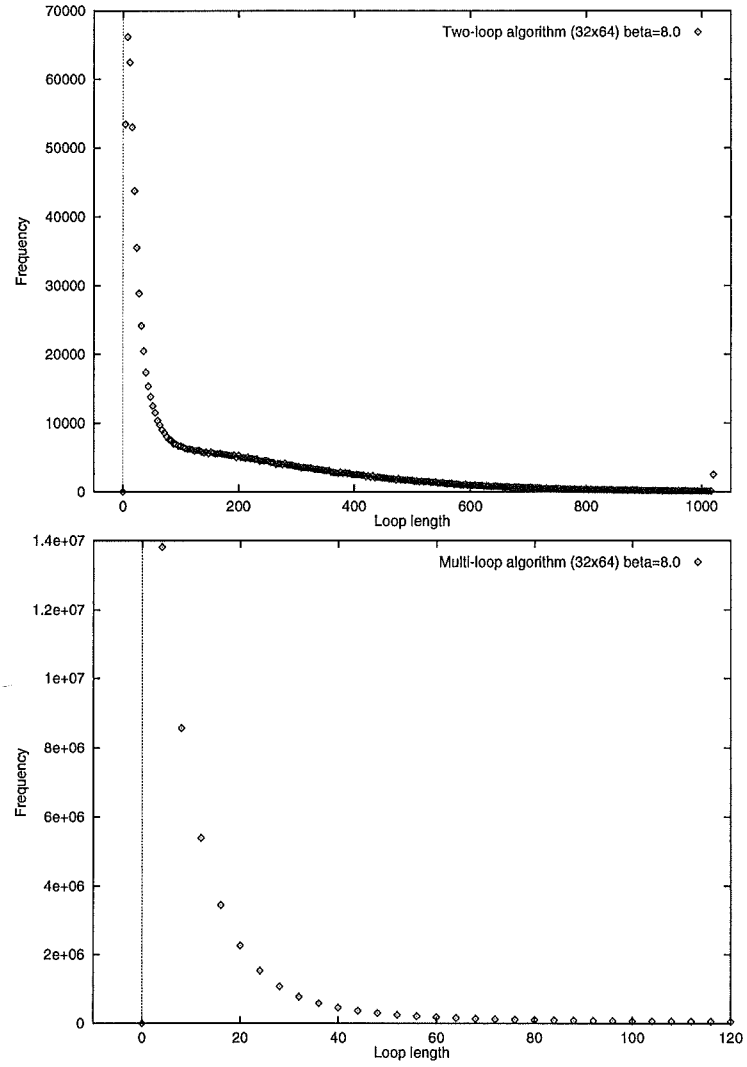

Figure 3-10: Loop statistics comparison between 2-loop algorithm and multi-loop algorithm

In the study of the specific heat, it is noticed that the two-loop algorithm does not converge as fast as the multi-loop algorithm, even after we take into account the fact that the two-loop version takes less time in doing one cycle of computation. Based

on the difference of the loop statistics, this could be an indication that specific heat depends very much on smaller loops rather than depends mainly on larger ones.

Chapter 4

Conclusion

In this paper, we have demonstrated how to use the loop cluster algorithms to study quantum spin$\frac{1}{2}$ systems. Improved estimator is constructed for the specific heat together with those for the susceptibility and the internal energy density.

The simulations give results that are in agreement with theoretical predictions and data from earlier studies using different approaches.

When the algorithm is pushed to the low temperature limit, these discrete Euclidean time methods encounter significant difficulty as simulation time goes up dramatically for the same data accuracies and memory storage.

If the improved estimator formulation can be combined with a continuous Euclidean time method[4], then the trouble with the large $2N$ requirement is eliminated completely. There is high hope that the low temperature characteristics of quantum spin chains can be studied without much difficulty with such an algorithm equipped with the improved estimators.

Bibliography

[1] A. Furusaki, M. Sigrist, E. Westerberg, and P.A. Lee *Random Exchange Quantum Heisenberg Chains* 1996.

[2] U.-J. Wiese and H.-P. Ying, Phys. Lett. A 168, 143 (1992).

[3] U.-J. Wiese and H.-P. Ying, Z. Phys. B 93, 147 (1994).

[4] B.B. Beard and U.-J. Wiese, *Simulations of Discrete Quantum Systems in Continuous Euclidean Time* 1996.

[5] U.-J. Wiese, *A Pathintegral Formulation of Quantum Spin Systems* pre-print.

[6] M. Hasenbusch, *An Improved Estimator for the Correlation Function of 2D Nonlinear Sigma Models* 1994